JOURNAL OF CATALYSIS **152**, 122–129 (1995)

Reactant Adsorption and Its Impact upon MTBE Synthesis on Zeolites

A. Kogelbauer, A. A. Nikolopoulos, J. G. Goodwin, Jr.,[1] and G. Marcelin

Department of Chemical and Petroleum Engineering, University of Pittsburgh, Pittsburgh, Pennsylvania 15261

Received May 23, 1994; revised October 11, 1994

Zeolites show interesting properties as catalysts for MTBE synthesis from methanol and isobutene such as a high selectivity to MTBE even at a low methanol/isobutene feed ratio. In order to explain this high selectivity, the adsorption behaviors of HY and HZSM-5 zeolites and their impact on activity and selectivity for MTBE synthesis were studied. Adsorption experiments, carried out under conditions similar to those used for reaction, showed that ca. 2.5 molecules of methanol were adsorbed per acid site on HZSM-5 and HY zeolites, whereas isobutene was found to form a 1:1 adsorption complex. The excess methanol adsorbed was found to be only weakly bonded, probably *via* hydrogen bonds. On a commercially used resin catalyst (Amberlyst-15) equal amounts of methanol and isobutene were adsorbed. The higher methanol uptake of the zeolites was paralleled by a higher selectivity to MTBE as compared to the resin catalyst. The increased adsorption of methanol on the zeolites was concluded to play a key role in suppressing the formation of by-products due to isobutene dimerization or oligomerization by decreasing the adsorption of isobutene on the active sites and thereby keeping these sites available for reaction.

INTRODUCTION

During the past decade, MTBE (methyl *tert*-butyl ether) has become heavily utilized as a quality-improving additive for gasolines. MTBE has become the additive of choice in the United States to meet the quality standards imposed upon gasoline by the Clean Air Act Amendments (1) due to its advantageous properties with respect to environmental concerns during the engine combustion process (2). Because of restrictions in the applicability of the resin catalyst currently used in the commercial synthesis of MTBE (3), considerable effort has been focused on the search for a suitable alternative catalyst. Apart from their excellent stability at elevated temperatures, zeolites show high selectivities toward MTBE even for methanol/isobutene feed ratios less than 1 (4), contrary to what is seen for the commercial resin catalysts. This could be of substantial interest for the commercial synthesis process, where higher methanol/isobutene ratios have to be used, hence increasing the costs due to separation and recycling of the excess methanol. In the case of HZSM-5, the high selectivity has been suggested to result from some sort of shape selectivity (4). Recent results obtained by our group (5) with HY zeolites indicate that causes other than mere spatial constraints may play a role. Chu and Kühl (4) have also reported unexpectedly high MTBE selectivity for rare earth exchanged HY zeolites and suggested that preferential adsorption of methanol on the more polar HY zeolite may be the cause. In order to clarify this point, the adsorption behavior of the reactants on HY, HZSM-5, and Amberlyst-15 have been studied under conditions similar to those used for reaction.

EXPERIMENTAL

The catalysts used in this study were zeolites of types HZSM-5 (Mobil) and HY (LZ210-12, UOP) as well as the commercially used Amberlyst-15 ion-exchange resin (Rohm & Haas). Characteristics of these catalysts are given in Table 1.

The adsorption measurements were carried out in a fixed-bed flow reactor system (5) using a transient technique (6) in which the concentration of an adsorbate in the reactor effluent was monitored as a function of time. UHP helium was used as an inert carrier gas. Isobutene (liquefied) was supplied from a pressurized tank by evaporation. Methanol was fed by bubbling helium through an isothermal saturator (32 ± 0.5°C). All gas flow rates were kept constant using mass flow controllers.

Typically, 25 mg of catalyst was activated under flowing helium by heating at a rate of 2°C/min to 400°C (105°C for Amberlyst-15) and maintaining this temperature for 12 h. After the catalyst had cooled to the desired adsorption temperature (100°C), the partial pressure of the adsorbate was increased *via* a step change by replacing the pure helium flow with a premixed isobutene/helium (methanol/helium) flow using a six-port valve. The transient response of the system was monitored using an on-

---

[1] To whom correspondence should be addressed.

0021-9517/95 $6.00

TABLE 1

Characteristics of the Catalysts

	Si/Al	Concentration of acid sites (mmol/g)[a]	Pore volume (cm^3/g)[b]
HZSM-5	12	1.2	0.20
HY	6	1.7	0.33[c]
Amberlyst-15	—	4.9	0.48

[a] Determined by the number of lattice aluminum atoms for HZSM-5 and by pyridine TPD for HY; for Amberlyst-15 see Ref. (13).

[b] For HZSM-5 see Ref. (11), for HY see Ref. (40), and for Amberlyst-15 see Ref. (12).

[c] Corresponds to the volume of the supercages.

line FID. In such an experiment the adsorbate is retained in the reaction system due to two effects: (i) the time required to pass the void volume of the reactor system (gas-phase holdup) and (ii) a delay caused by the interaction of the adsorbate with the catalyst (adsorption). Nonideal plug flow behavior additionally broadens the transient curve due to axial diffusion effects. Normalization and integration of the transient curve give the retention time of the adsorbate. Multiplication of this retention time by the molar flow rate provides the retained amount of adsorbate. In order to correct for gas-phase holdup and diffusional effects, transients with weakly interacting (nonchemisorbing) compounds of similar structure, methane and isobutane, were recorded and subtracted from the curves obtained with methanol and isobutene as adsorbates. The retention times for these weakly interacting compounds were virtually identical with those obtained from blank runs carried out with methanol and isobutene using identical flows and quartz sand as the catalyst bed. The reproducibilities of the single transients were better than ±5%.

After the adsorption step, the samples were flushed with helium for 1 h at 100°C to remove weakly adsorbed molecules. Subsequent temperature-programmed desorption in helium flow up to 350°C at a heating rate of 10°C/min was performed in order to assess the amount of strongly-bound adsorbate. Since the accuracy of these measurements may be influenced by the formation of nondesorbing carbonaceous species (such as those due to dimerization of isobutene), the strongly adsorbed amount was also determined by the following procedure. After the first transient the catalyst was purged with helium for 1 h at 100°C to remove the weakly-bound adsorbate. Subsequently a second transient identical to the first adsorption step was carried out. The quantity determined from the second transient corresponded to the amount of weakly adsorbed reactants. The quantity of strongly adsorbed reactants was obtained by the difference between the amounts determined from the first and the second transient. Repeating this procedure provided a measure of the accuracy for the determination of the weakly adsorbed species.

In a separate set of experiments the transients were monitored by injecting samples of the reactor effluent periodically using a six-port valve equipped with a sample loop into a GC with a Porapak-Q column and FID. This procedure was carried out to check for possible reaction products formed during the adsorption transients.

Catalytic reactions were carried out in a flow microreaction system using a 6-mm quartz glass U-tube as reactor. The system was equipped with mass flow meters, a back pressure regulator, and temperature controllers allowing precise control of the flow, the partial pressure of all reactants, and the line and furnace temperatures (±0.5°C). Methanol (Aldrich, A.C.S. HPLC grade) was fed by bubbling helium (99.999%) through a jacketed saturator. Isobutene was obtained from Liquid Carbonic as a 10% mixture in helium. No constituents other than isobutene were observed in a GC analysis of this gas mixture. For experiments requiring higher isobutene feed concentrations, liquefied isobutene was evaporated from a pressurized tank. Catalyst samples of ca. 25 mg were heated under flowing helium at 2°C/min to 400°C (105°C for Amberlyst-15) and kept at that temperature for 12 h in order to activate them. After cooling to the desired reaction temperature, constant flows of methanol, isobutene, and helium were fed at atmospheric pressure with reaction reaching steady state typically in ca. 2 h. Samples of the reactor effluent were injected into a GC by means of a sampling valve and analyzed using a Porapak-Q column and an FID. Conversions were kept below 10% in order to maintain differential reaction. In order to test catalyst selectivity at low methanol/isobutene ratio and to observe appreciable amounts of products (both MTBE and isobutene dimers), the reaction was carried out between 70 and 150°C using a reactant feed of methanol (14 mol%) and isobutene (28 mol%) diluted with helium. Apparent energies of activation for MTBE formation were determined in a temperature range between 70 and 100°C to check for equilibrium and transport limitations (7). Selectivities were calculated on a molar basis.

In order to elucidate the impact of reactant adsorption upon MTBE formation, adsorption of the reactants (methanol and isobutene) was carried out prior to reaction in separate experiments. For these experiments, the catalysts were initially contacted with a flow containing helium and one of the reactants at 90°C for 30 min. Then both reactants were admitted at a reactant feed ratio of 1 (4.4 mol% each, helium balance). Catalyst activity was recorded over a period of 1.5 h. Afterwards, the catalyst was subjected to a heat treatment under helium (400°C for 2 h), and then the preadsorption/reaction cycle as described above was repeated. This regeneration treatment was sufficient to restore the catalytic activity to its original value following reaction after preadsorption of isobutene where strong deactivation was observed.

RESULTS

The transients obtained for the adsorption of methanol and isobutene on HY zeolite at 100°C are shown in Fig. 1 and in Fig. 2, respectively. Similar transients were obtained for the other catalysts. As can be seen from Fig. 1, the transient responses for the second and third adsorption steps (both after an intermediate purge with helium at 100°C for 1 h) were essentially identical and demonstrated the good reproducibility for the adsorption of weakly bound methanol. Based on the areas between the transient curves, the amount of strongly adsorbed methanol was less than that weakly adsorbed. The amount of weakly adsorbed isobutene (Fig. 2) seemed to be very small since the transient curve for the adsorption step after intermediate He purge at 100°C almost coincided with that of the blank run. We conclude therefore that isobutene was not able to desorb easily from the catalyst surface at 100°C either due to its being strongly adsorbed or due to the formation of reaction products incapable of desorption at a temperature this low.

The results of the adsorption studies are compiled in Table 2 for methanol and in Table 3 for isobutene. In addition to the absolute amount of adsorbate, the corresponding liquid volume assuming the adsorbates to be in the liquid state at 100°C, the fraction of the zeolite pores filled assuming liquid adsorbate, and the number of molecules adsorbed per acid site were calculated. This additional information aids in better understanding how the molecules are bound to the catalyst surface and indicates the extent of transport limitations expected. Comparing the absolute amounts of adsorbed methanol and isobutene, it is obvious that the zeolites were able to adsorb much more methanol than isobutene, whereas Amberlyst-15 adsorbed almost equal amounts of both adsorbates. This behavior becomes more understandable when the site coverages are taken into account. On the zeolites, approximately 1 molecule of isobutene adsorbed per acid site, whereas ca. 2.5 molecules of methanol adsorbed per acid site. The large amount of adsorbed meth-

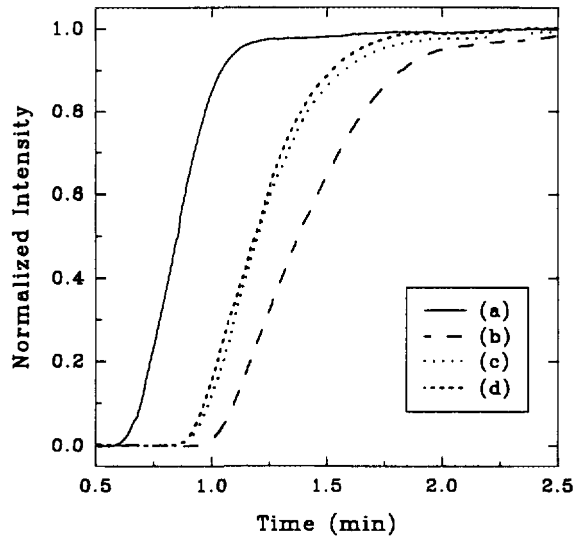

FIG. 1. Typical transient response during adsorption of methanol on HY zeolite at 100°C [(a) blank, (b) first adsorption step, (c) second adsorption step, and (d) third adsorption step after intermediate He purges at 100°C for 1 h].

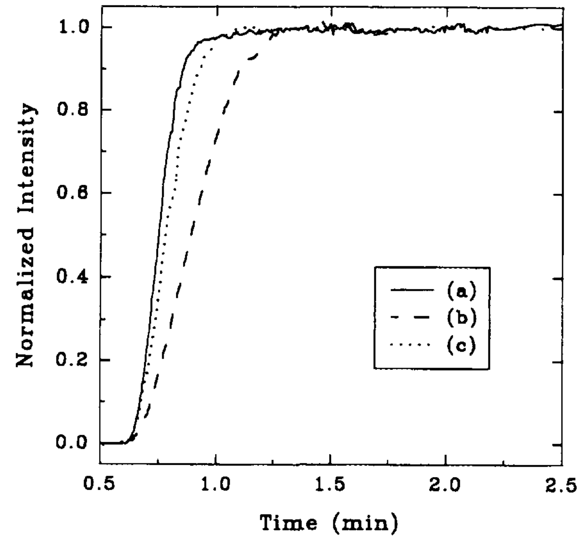

FIG. 2. Typical transient response during adsorption of isobutene on HY zeolite at 100°C [(a) blank, (b) first adsorption step, and (c) second adsorption step after intermediate He purges at 100°C for 1 h].

TABLE 2

Adsorption of Methanol at 100°C and $P_{MeOH,i}$ = 15 kPa

	Adsorbed amount (mmol/g)	Total molecules adsorbed per acid site	Liquid amount[a] (cm³/g)	Pore fraction filled[b] (%)	Molecules desorbed per acid site (100–350°C)[c]
HZSM-5	3.2	2.6	0.15	75	0.8
HY	3.7	2.2	0.17	52	1.5
Amberlyst	1.2	0.3	0.05	10	NM[d]

[a] Calculated based on the density of the liquid at 100°C under its vapor pressure.

[b] Assuming estimated liquid amount in pores.

[c] Corresponds to strongly adsorbed methanol.

[d] Not measured due to thermal instability of the catalyst.

TABLE 3

Adsorption of Isobutene at 100°C and $P_{IB,i}$ = 30 kPa

	Adsorbed amount (mmol/g)	Total molecules adsorbed per acid site	Liquid amount[a] (cm^3/g)	Pore fraction filled[b] (%)	Molecules desorbed per acid site (100–350°C)[c]
HZSM-5	1.2	1.0	0.14	70	0.6
HY	1.5	0.9	0.17	52	0.8
Amberlyst	1.3	0.3	0.15	31	NM[d]

[a] Calculated based on the density of the liquid at 100°C under its vapor pressure.

[b] Assuming estimated liquid amount in pores.

[c] Corresponds to strongly adsorbed isobutene.

[d] Not measured due to thermal instability of the catalyst.

anol can be attributed to the formation of clusters of adsorbed methanol, which has been described for other zeolites (8–11). On the contrary, Amberlyst-15 did not form a 1 : 1 adsorbate–site complex with either methanol or isobutene. On average 1 molecule adsorbed for each adsorbate per three adsorption sites.

Although the fraction of the pore volume that was filled, assuming the adsorbates to be in the liquid state, was relatively high for HZSM-5 (70–75%), only 50% of the accessible volume (volume of the supercages) was filled for HY. This indicates that, although the pore volume represents an upper limit for the amount of adsorbed molecules, it did not seem to be the limiting factor for the size of the methanol clusters. Nevertheless, the extent of the pore filling might lead to the expectation of internal transport limitations particularly with HZSM-5. It should be noted that the values for the filled pore fraction for Amberlyst-15 are not very meaningful since it has an average pore diameter of around 300 Å (12, 13), indicating rather large and shallow pores very similar to those of nonmicroporous, high-surface-area catalysts.

TPD of the adsorbates from the zeolites after adsorption showed that, in the temperature range between 100 and 350°C, amounts equivalent to 0.8 and 1.5 molecules of methanol per acid site desorbed from HZSM-5 and from HY, respectively. The corresponding values for desorbed isobutene were 0.6 and 0.8 molecules per accessible acid site of HZSM-5 and of HY, respectively. Since the amount desorbing during TPD corresponds to strongly chemisorbed species, the results suggest that both methanol and isobutene form ca. 1 : 1 adsorbate–site complexes on the zeolites in which the adsorbate molecule is strongly bound, most probably protonated. Due to the limited thermal stability of the resin, TPD could not be carried out for it after adsorption.

The differences in adsorption behavior between the zeolites and Amberlyst-15 were also reflected in their catalytic performances for MTBE synthesis. Figure 3 shows the catalyst selectivity to the major reaction by-products, the isobutene dimers (2,4,4-trimethyl-1-pentene and 2,4,4-trimethyl-2-pentene) as a function of reaction temperature at a methanol/isobutene feed ratio of 0.5. Both zeolites, HY and HZSM-5, exhibited significantly lower selectivities to isobutene dimers than the resin catalyst in the temperature range between 60 and 100°C. Note that despite the excess of isobutene in the reactant feed the zeolites apparently did not form significant amounts of isobutene dimers at temperatures below 100°C. At 100°C, at which the extent of MTBE formation was limited by thermodynamic equilibrium for both HZSM-5 and Amberlyst-15 under the experimental conditions used (14), the resin catalyst exhibited around 25% selectivity to isobutene dimers compared to approximately 1% for the zeolite. This indicates that the higher selectivity to isobutene dimers observed with Amberlyst-15 was not caused by a limitation of the rate of formation of MTBE by thermodynamic equilibrium but rather by a higher intrinsic rate of isobutene dimerization on Amberlyst-15.

This is more clearly illustrated in Fig. 4, which shows the temperature dependence of the rates of isobutene dimerization during MTBE synthesis in the form of an Arrhenius plot. At 100°C, the resin catalyst was about two orders of magnitude more active than the zeolites for dimer production. The TOFs for the dimerization were determined as 2 × 10^{-5} s^{-1} for the zeolites and 1.3 × 10^{-3} s^{-1} for the resin catalyst using the site concentration from Table 1. The apparent energies of activation were 41, 62, and 70 kJ/mol for the resin catalyst, HZSM-5, and HY, respectively. Calculations of equilibrium conversion

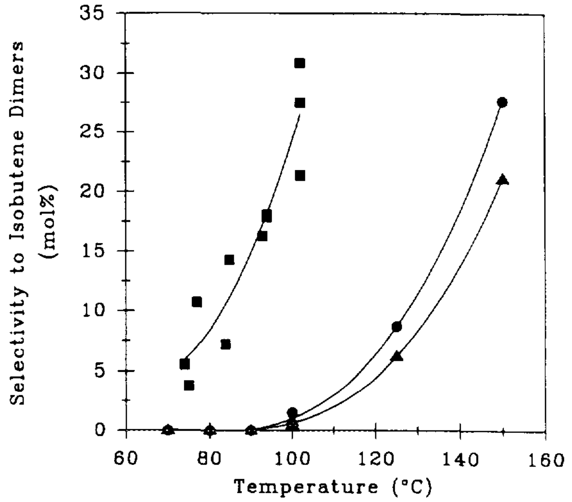

FIG. 3. Selectivity of acid catalysts to isobutene dimers during MTBE synthesis as a function of temperature (MeOH : IB = 0.5, P_{IB} = 28 kPa, WHSV = 20 h^{-1}): (●) HY, (▲) HZSM-5, (■) Amberlyst-15.

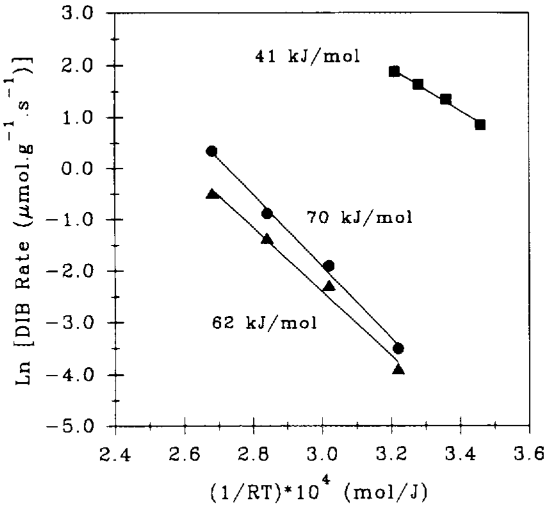

FIG. 4. Rate of isobutene dimerization during MTBE synthesis as a function of temperature on acid catalysts (MeOH : IB = 0.5, P_{IB} = 28 kPa, WHSV = 20 h^{-1}): (●) HY, (▲) HZSM-5, (■) Amberlyst-15.

based on standard thermodynamic data indicated that isobutene dimerization was not limited by thermodynamic equilibrium at 100°C during these experiments (14).

The results for MTBE synthesis on HY after reactant preadsorption are shown in Fig. 5. In the first stage, reaction was carried out after preadsorption of methanol (squares). The catalyst was then purged with helium at 100°C for 1 h. In the second stage, reaction was carried out after preadsorption of isobutene (circles). Subsequently, the catalyst was regenerated with helium at 400°C for 2 h. Finally, reaction was carried out after preadsorption of methanol once again (diamonds). For comparison purposes, the results of a separate experiment in which both reactants were admitted simultaneously without preadsorption are included (triangles). Under the conditions of these experiments only MTBE was observed as a reaction product in the gas phase. The rate of reaction after methanol preadsorption (squares) was approximately double that without any preadsorption (triangles). The reaction rates were essentially constant with no significant deactivation during a period of 2 h. Isobutene preadsorption, however, had a dramatic effect upon catalyst performance as can be seen by the drop in activity by about one order of magnitude (circles) from that after methanol preadsorption (squares). Again, deactivation of the catalyst did not occur during a period of 2 h. The regeneration treatment (helium at 400°C for 2 h), however, completely restored catalyst activity as can be seen from the results for MTBE reaction after regeneration in helium and subsequent methanol preadsorption (diamonds). This indicates that strongly adsorbed isobutene-derived species were responsible for the decreased activity after isobutene preadsorption. These species were able to be removed under a helium flow at 400°C, suggesting that isobutene did not form coke at 90°C.

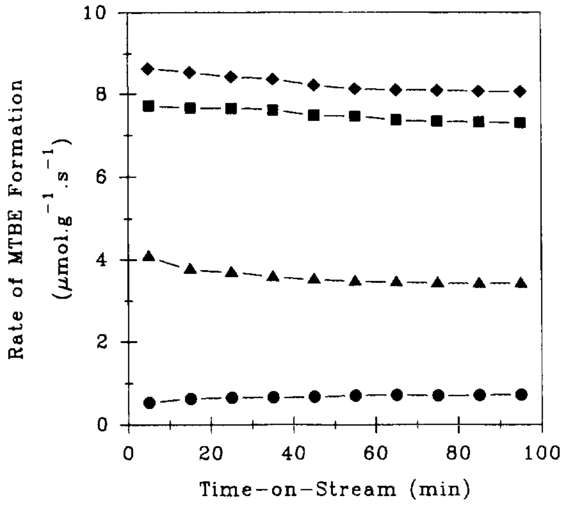

FIG. 5. Effect of reactant preadsorption upon MTBE synthesis activity of the HY zeolite (MeOH : IB = 1, P_{IB} = 6.9 kPa, T = 90°C) [reaction after preadsorption of (▲) nothing, (■) MeOH, (●) IB after regeneration in He at 100°C, (◆) MeOH after regeneration in He at 400°C].

DISCUSSION

The results of the adsorption experiments indicate that, at a temperature of 100°C and a partial pressure of 20 kPa, ca. 2.5 molecules of methanol are adsorbed on the average per acid site on the zeolites. On the other hand approximately 1 molecule desorbed per acid site during TPD, suggesting a coverage of roughly 1 strongly bound molecule of methanol per acid site. This number corresponds well with the results of Aronson *et al.* (11), who measured the adsorption of various alcohols on H-zeolites. It has been suggested (9, 11, 15) that this adsorption state corresponds to an ion pair of a methoxonium ion (a protonated methanol molecule) adsorbed on a SiOAl$^-$ zeolite lattice fragment.

The excess weakly-bound methanol can be accounted for as follows. As we pointed out earlier, it has been found that under suitable conditions methanol is able to form adsorption clusters on zeolites (9–11). This phenomenon is not limited to the H-form of zeolites. It has also been seen for alkali zeolites (9, 10), which implies that it reflects a property of polar adsorbate molecules, namely the ability to form mutual hydrogen bonds, rather than a specific zeolite–adsorbate interaction. It should be noted that the amounts of strongly adsorbed methanol and isobutene are roughly equal for each of the catalysts and that it is the weakly-bound excess methanol found during adsorption experiments which forms clusters *via* hydrogen bonds. It has been concluded that all hydrogen bonds of such clusters in HZSM-5 are equivalent and that the average strength of the hydrogen bonds decreases with increasing cluster size (9). This is consistent with a model in which dissipation of the positive charge of the proton over the whole adsorption cluster occurs, thereby delocalizing the charge of the original methoxonium ion. The close vicinity of lattice oxygen in the zeolites may further stabilize such adsorption clusters by providing additional sites for interaction through hydrogen bonds. The importance of the lattice oxygen of zeolites as additional adsorption sites for polar molecules has been emphasized in a number of papers in the literature (16–18).

Isobutene cannot form strong mutual hydrogen bonds and, thus, would not be expected to form adsorption clusters. This is very well reflected in the formation of only a 1 : 1 adsorbate–site complex on the zeolites. Judging from the strength of adsorption for isobutene, the formation of an adsorbate structure with proton transfer (protonated isobutene carbocation) is most probable, although other adsorption structures such as covalently bonded alkyl silyl ether (19, 20) and isobutene hydrogen bonded to the acid sites of the zeolite (21) have also been suggested. Due to their high reactivity (isobutene readily oligomerizes on zeolites at room temperature), adsorbed *tert*-butyl carbocations would not be easily observable by standard characterization techniques such as IR (22) or ^{13}C MAS–NMR spectroscopy (21). In any case, all the above proposed species have been shown to exhibit typical carbocation chemistry at elevated temperatures.

On Amberlyst-15 a 1 : 3 coverage of acid sites by adsorbate molecules was obtained. An incomplete coverage of the surface ($\theta < 1$), which could account for this finding, seems unlikely since it has been reported that the sites of Amberlyst-15 exhibit high uniform strength (23) and are at least as strong as those of zeolites (24). Also a comparison of the equilibrium constants of adsorption determined by modeling gas-phase reaction data for MTBE synthesis with Langmuir–Hinshelwood–Hougen–Watson kinetics on Ti-silicalites (25) and Amberlyst-15 (26) has revealed similar values. If all sites were not accessible, however, one would also expect an apparent lower coverage. Thus, incomplete swelling of the resin catalyst during the adsorption experiments from the gas phase could account for the lower coverage due to the inaccessibility of some sites.

Under our reaction conditions, no preferential uptake of methanol occurred on Amberlyst-15, which initially seems to be in contradiction with other reports. From kinetic analyses of MTBE formation (26) and MTBE decomposition (27), the adsorption constant calculated for methanol was approximately 10-fold higher than that calculated for isobutene, and Rehfinger and Hoffmann (28) observed highly selective methanol uptake into the micro gel phase of Amberlyst-15 beads (they reported a factor of 3.5 higher methanol uptake than *n*-butane uptake from pure liquids; however, no absolute numbers concerning the coverage of sulfonic acid groups by reactant molecules were reported). Since the preferential uptake of methanol and other polar substances is linked to the swelling and penetration of the polymer matrix our results suggest that adsorption occurred mainly on easily accessible, nonselective sites on or near the surface. Thus, the relation of intrinsic reaction rates and the rate of transport of the alcohol into the gel phase becomes a key issue in understanding the selectivity behavior of the resin catalyst.

In a series of papers, Rehfinger and Hoffmann (28–30) investigated the kinetics of the liquid-phase MTBE synthesis on Amberlyst-15 and came up with some interesting results. First, they demonstrated that transport phenomena, particularly macropore diffusion of methanol, can significantly impact upon the reaction and thus alter macroscopically measured reaction rates, activation energies, and reaction orders, as well as shift selectivities to isobutene dimers. They suggested a shell–core model in which the outer shell of a resin bead exclusively formed MTBE while the core formed the olefin dimer. Iborra *et al.* (13) observed notable differences in the normalized reaction rates (TOF based on surface area or sites) of ETBE formation on sulfonated macroporous resin catalysts having different degrees of crosslinking. They concluded that permeation of reactants into the polymer matrix was limiting the reaction rates. It was additionally reported that at high temperatures adsorption was weak and the reaction rate was fast enough to make permeation so slow that actually it was not observed (31). The process parameters used in our reaction and adsorption experiments definitely favor limitations due to slow permeation for the resin because we applied relatively high temperatures (100°C), a low methanol/isobutene ratio (0.5), and low reactant (adsorbate) partial pressures (14 and 28 kPa). However, they were chosen deliberately to avoid transport and equilibrium limitations on the zeolites and to have a worst-case scenario in terms of isobutene dimer selectivities. Regarding our data in this light, the results are in agreement with what was reported in the literature.

Although we have no data on the simultaneous adsorption behavior of methanol and isobutene due to the impossibility of preventing reaction under these conditions, it is reasonable to assume that the higher affinity of zeolites for methanol is also reflected in a higher methanol coverage under reaction conditions. Since we observed significant differences in the selectivity of the MTBE synthesis reaction on zeolites and Amberlyst-15 and since the selectivities of the zeolites have been reported to be relatively insensitive to the reactant ratio (4), these two phenomena seem to be closely related.

Until now, the superior selectivity of zeolites towards MTBE has been attributed to the shape selectivity of zeolites (4). In the case of MTBE synthesis this would mean either that isobutene dimers cannot be formed within the confined space of a zeolite pore (*transition state selectivity*) or that already formed isobutene dimers cannot diffuse out of the zeolite pore at a fast enough rate (*product selectivity*) using the definitions for shape selectivity as given in (32). HZSM-5 is known to exhibit shape selectivity for some reactions such as xylene isomerization (33), and the dimensions of the zeolite channels (5.4 × 5.6 Å) are definitely in the range where *product selectivity* might be expected. For HY on the other hand, pore openings (7.4 × 7.4 Å) as well as the diameter of the supercage (11 Å) make this possibility very unlikely. Although the remaining accessible volume inside the pores of HY might be significantly reduced due to the adsorption of reactants, as indicated by pore filling of approximately 50% during adsorption of the single compounds, neither of the two mechanisms leading to shape selectivity can account for the observations of the reaction experiments after reactant preadsorption. The fact that methanol preadsorption increased the rate of reaction compared to that in experiments in which both reactants were initially admitted simultaneously is a strong argument against spatial constraints induced by reactant adsorption. Additional support for the absence of *product selectivity* for at least HY is found from the comparison of the values of the apparent energies of activation for isobutene dimerization. The value of 41 kJ/mol determined for Amberlyst-15 is very close to the value reported by Rehfinger and Hoffmann (30), who concluded that gel-phase diffusion affected their reaction rates. The value of 70 kJ/mol for HY is much closer to the value obtained by Haag (34) using Amberlyst and to the 81.7 kJ/mol reported by Ngandjui and Thyrion (35) using H-mordenite for the oligomerization of isobutene in the absence of transport limitations as indicated by an absence of crystallite size effects. The value of the apparent energy of activation together with the fact that we are dealing with low-temperature reaction data and a perfectly straight Arrhenius plot can be taken as an indication for the absence of mass transport limitations in the case of HY. For HZSM-5, however, we cannot exclude at least some impact of mass transport limitations.

Since the preadsorption of isobutene showed a detrimental effect upon rates of MTBE formation without altering the selectivity and the preadsorption of methanol showed the opposite, methanol is concluded to have some sort of protective functionality in MTBE synthesis. The reduction in reaction rate as a consequence of isobutene adsorption occurred immediately, persisted over a 2-h reaction period, and could be removed only by heat treatment at 400°C in an inert gas flow. This behavior is indicative of a poisoning mechanism by a strongly adsorbed species which could be either adsorbed isobutene itself or dimerization/oligomerization products of isobutene. If we consider strongly chemisorbed isobutene to be responsible for the site blocking, it must also be considered relatively inert toward reaction since no noticeable increase in the MTBE formation rate was observed with time-on-stream once methanol was admitted to the catalyst after isobutene preadsorption (see circles in Fig. 5). This has significant consequences for the mechanism of the etherification reaction because it would indicate that MTBE cannot be formed by the reaction of chemisorbed (protonated) isobutene and methanol. That is, however, in contradiction to a variety of studies using different catalysts and reaction media (36) and to the proposed mechanism for the homogeneous-phase reaction (37) in which the reaction of protonated isobutene with methanol has been suggested. It seems, thus, more plausible that isobutene dimers, once formed, block the acid sites of the zeolites. With regard to these conclusions, the adsorption of methanol becomes a key role for MTBE synthesis, although in exactly what way is not completely understood yet. Note that the high activity of the catalyst after methanol preadsorption was maintained for a period of almost 2 h with only minute deactivation, indicating that once methanol is adsorbed it remains effectively in the zeolite pores and is not easily replaced. Methanol is believed to protect the acid sites from isobutene adsorption by decreasing the isobutene concentration near an acid site, thereby reducing the probability for dimer formation, by acting as protonating agent itself, thus making the proton transfer to the olefin the rate-limiting step, or by a combination of both. A similar effect, suppression of the rate of isobutene dimerization by addition of methanol and MTBE, has been reported recently for Lewatit K-2631, a sulfonated resin catalyst similar to the one used in our study (38).

The existence of two complementary mechanisms for the formation of MTBE from isobutene and methanol has been claimed by Ancillotti *et al.* (39) for the liquid-phase synthesis of MTBE on Amberlyst-15. They proposed that a very efficient concerted mechanism (in which protonated isobutene reacts with methanol) is prevalent at low methanol-to-isobutene feed ratios (<0.1) and that a less efficient ionic mechanism (in which a methoxonium ion acts as proton donor) is dominant for methanol-to-isobutene ratios of 2 and higher. Although the data presented in this work do not enable us to differentiate between the two possible routes unequivocally, our results favor the reaction pathway in which adsorbed methanol acts as a protonating agent.

CONCLUSIONS

Adsorption experiments under conditions similar to those used for reaction showed that on zeolites approximately 2.5 molecules of methanol were adsorbed per acid site, whereas isobutene adsorption reached a coverage of only one molecule per acid site. On Amberlyst-15 equal amounts of methanol and isobutene were adsorbed. This and the lower coverage of ca. 1 adsorbate molecule per three acid sites were attributed to the slow permeation of reactants into the gel phase of Amberlyst-15 under our reaction conditions. The higher methanol coverage on the zeolites as determined by adsorption was paralleled by an increased selectivity to MTBE. Reactant adsorption prior to reaction showed that adsorption of isobutene leads to site poisoning most likely due to strongly bound isobutene dimers. Excess methanol present in the zeolite pores was concluded to effectively protect the acid sites from isobutene adsorption, thus preserving the concentration of active sites accessible during reaction. The presence of lattice oxygen in the zeolite channels is considered to be responsible possibly for the higher methanol concentration in the zeolites.

ACKNOWLEDGMENTS

Funding for this research from the Materials Research Center of the University of Pittsburgh through AFOSR Grant 91-0441 is gratefully acknowledged. The assistance of Dr. Xinrui Xia with some of the adsorption experiments is also appreciated.

REFERENCES

1. Peeples, J. E., *Fuel Reformulation* **1**(1), 27 (1991).
2. Piel, W. J., and Thomas, R. X., *Hydrocarbon Process.* **69**(7), 68 (1990).
3. Takesono, T., and Fujiwara, Y., U. S. Patent 4,182,913 1980.
4. Chu, P., and Kühl, G. H., *Ind. Eng. Chem. Res.* **26**, 366 (1987).
5. Nikolopoulos, A. A., Oukaci, R., Goodwin, J. G., Jr., and Marcelin, G., *Prepr. Div. Pet. Chem., Am. Chem. Soc.* **37**(3), 787 (1992).
6. Efstathiou, A. M., Suib, S. L., and Bennett, C. O., *J. Catal.* **131**, 94 (1991).
7. Nikolopoulos, A. A., Kogelbauer, A., Goodwin, J. G., Jr., and Marcelin, G., *Appl. Catal. A* **119**, 69 (1994).
8. Mirth, G., and Lercher, J. A., *in* "Natural Gas Conversion" (A. Holmen *et al.*, Eds.), p. 437. Elsevier, Amsterdam, 1991.
9. Mirth, G., Lercher, J. A., Anderson, M. W., and Klinowski, J., *J. Chem. Soc. Faraday Trans.* **86** (17), 3039 (1990).
10. Kogelbauer, A., and Lercher, J. A., *J. Chem. Soc. Faraday Trans.* **88** (15), 2283 (1992).
11. Aronson, M. T., Gorte, R. J., and Farneth, W. E., *J. Catal.* **98**, 434 (1986).
12. Marcelin, G., Cronauer, D. C., Vogel, R. F., Prudich, M. E., and Solash, J., *Ind. Eng. Chem. Process Des. Dev.* **25**, 747 (1986).
13. Iborra, M., Tejero, J., Izquierdo, J. F., and Cunill, F., *Br. Polym. J.* **23**, 117 (1990).
14. Nikolopoulos, A. A., Oukaci, R., Goodwin, J. G., Jr., and Marcelin, G., *Catal. Lett.* **27**, 149 (1994).
15. Kubelkova, L., Novakova, J., and Nedomova, K., *J. Catal.* **124**, 441 (1990).
16. Senkyr, G., and Noller H., *J. Chem. Soc. Faraday Trans.* **71**, 997 (1975).
17. Salvador, P., and Kladnig, W., *J. Chem. Soc. Faraday Trans.* **73**, 1153 (1977).
18. Mirth, G., Kogelbauer, A., and Lercher, J. A., *in* "Proceedings from the Ninth International Zeolite Conference Vol. II" (R. von Ballmoos, J. B. Higgins, and M. M. J. Treacy, Eds.), p. 251. Butterworth–Heinemann, Stoneham, 1993.
19. Aronson, M. T., Gorte, R. J., Farneth, W. E., and White, D., *J. Am. Chem. Soc.* **111**, 840 (1989).
20. Haw, F. J., Richardson, B. R., Oshiro, I. S., Lazo, N. D., and Speed, J. A., *J. Am. Chem. Soc.* **111**, 2052 (1989).
21. Lazo, N. D., Richardson, B. R., Schettler, P. D., White, J. L., Munson, E. J., and Haw, J. F., *J. Phys. Chem.* **95**, 9420 (1991).
22. Kogelbauer, A., Goodwin, J. G., Jr., and Lercher, J. A., in preparation.
23. Gates, B. C., and Rodriguez, W., *J. Catal.* **31**, 27 (1973).
24. Tau, L. M., and Davis, B. H., *Appl. Catal.* **53**, 263 (1989).
25. Chang, K. H., Kim, G. J., and Ahn W. S., *Ind. Eng. Chem. Res.* **31**, 125 (1992).
26. Tejero, J., Cunill, F., and Izquierdo, J. F., *Ind. Eng. Chem. Res.* **28**, 1269 (1989).
27. Cunill, F., Tejero, J., and Izquierdo, J. F., *Appl. Catal.* **34**, 341 (1987).
28. Rehfinger, A., and Hoffmann, U., *Chem. Eng. Sci.* **45** (6), 1605 (1990).
29. Rehfinger, A., and Hoffmann, U., *Chem. Eng. Sci.* **45** (6), 1619 (1990).
30. Rehfinger, A., and Hoffmann, U., *Chem. Eng. Technol.* **13**, 150 (1990).
31. Jerabek, K., *Collect. Czech. Chem. Commun.* **42**, 805 (1977).
32. Chen, N. Y., Garwood, W. E., and Dwyer, F. G., *in* "Shape Selective Catalysis in Industrial Applications." Dekker, New York, 1989.
33. Weisz, P. B., *Pure Appl. Chem.* **52**, 2091 (1980).
34. Haag, W. O., *Chem. Eng. Prog. Symp. Ser.* **63**, 140 (1967).
35. Ngandjui, T., and Thyrion, F. C., *Chem. Eng. Proc.* **31**, 1 (1992).
36. Hutchings, G. J., Nicolaides, C. P., and Scurrell, M. S., *Catal. Today* **15**, 23 (1992) and references therein.
37. Kemp, D. S., and Vellaccio, F., *in* "Organic Chemistry." p. 260. Worth, New York, 1980.
38. Izquierdo, J. F., Vila, M., Tejero, J., Cunill, F., and Iborra, M., *Appl. Catal. A* **106**, 155 (1993).
39. Ancillotti, F., Mauri, M. M., Pescarollo, E., and Romagnoni, L., *J. Mol. Catal.* **4**, 37 (1978).
40. Shertukde, P. V., Hall, W. K., and Marcelin, G., *Catal. Today* **15**, 491 (1992).